Intermolecular energy transfer in liquid water and its contribution to heat conduction: A molecular dynamics study

Intermolecular energy transfer in liquid water and its contribution to heat conduction: A molecular dynamics study

Taku Ohara[a)]

Institute of Fluid Science, Tohoku University, 2-1-1 Katahira, Aoba-ku, Sendai, 980-8577, Japan

Intermolecular energy transfer (IET) is a dominant factor in heat conduction in liquid. The IET in liquid water and its contribution to macroscopic heat conduction under a temperature gradient were analyzed by a molecular dynamics simulation utilizing the extended simple point charge (SPC/E) potential model. Intermolecular energy exchange rates (IEERs) for both the translational and rotational motion of molecules were defined and their characteristics examined. The IEER of hydrogen-bonded molecules and nonbonded molecules have different characteristics. The IEER oscillates with a high amplitude and its time average, which is much smaller than the magnitude of the IEER, gives the effective rate of the IET that contributes to macroscopic heat conduction. In the present study, the effective rate of the IET was assumed to be proportional to the magnitude of the IEER. Based on the characteristics of the IEER and the above supposition, contributions of the translational and rotational IET between hydrogen-bonded molecules and nonbonded molecules to macroscopic heat conduction were evaluated. The evaluated results were compared with the results of a molecular dynamics (MD) simulation of heat conduction under a constant temperature gradient, and good qualitative agreement between the predicted value and the simulated result was found. The rotational IET was found to be dominant as compared with the translational IET, and the contribution of hydrogen-bonded molecules to heat conduction was found to be relatively small. The possibility of a mechanism that cancels the IET between distant molecules and the development of a precise model for this mechanism were also discussed. © *1999 American Institute of Physics.* [S0021-9606(99)50138-4]

I. INTRODUCTION

The molecular mechanism of heat conduction in liquid is of fundamental interest in many areas of science and technology. In particular, understanding the mechanism and characteristics of heat conduction in water are important to the fields of thermal engineering, life, and environmental sciences. The significance of an understanding of the molecular mechanism is twofold. First, by understanding the mechanism that determines thermal conductivity, we will be able to predict the influence of temperature, density, and impurities, such as ions, on thermal conductivity. Second, aside from the macroscopic heat conduction in continuum fluid, we will have a greater understanding of the role of molecular-scale energy transfer in microscopic or nonequilibrium thermal phenomena. For example, the release of kinetic energy from incident molecules at the liquid–vapor interface determines the behavior of the molecules, which are either absorbed into the liquid phase or reflected back to the vapor phase. The characteristics of energy transfer at the solid–liquid interface, which determines the thermal phenomena of liquid-filled micropores and microchannels, are also of interest in nanotechnology. The transfer of nonequilibrium energy in a very short time, which is related to the ultrarapid heating of materials by using a laser, is of interest to scientists in the field of thermal engineering. Understanding the molecular mechanism of energy transfer in liquids will lead to new insights into these thermal phenomena and their practical applications where the continuum theory is no longer effective.

Heat conduction in low-density gases is mainly due to molecular motion, which transports the kinetic energy of molecules. Energy exchange between gas molecules occurs instantly at the moment of binary collision and these characteristics have also been identified in water.[1] On the other hand, in dense fluid, energy exchange between molecules occurs in the process of continuous interactions. Heat conduction is mainly due to the interaction between molecules, which is especially significant at low temperature. Molecular-scale structure is obvious in dense liquids, and it may influence the energy-transfer phenomenon.

A number of molecular dynamics (MD) studies have been reported[2–9] in which the thermal conductivity of pure liquids[2,3,5–8] and binary mixtures[3,4,9] is determined. The equilibrium MD[2–4] with the Green–Kubo formula or the nonequilibrium MD[5–9] were applied in these studies. Most of the studies[2–5,8,9] are for simple liquids modeled by the Lennard-Jones potential, but some studies[6,7] include polyatomic molecules and consider the rotational motion of molecules. There was good agreement among the studies for simple liquids, and the basic method to calculate the thermal conductivity by MD simulations appears to be established. However, to the best of our knowledge, there have been no reports in which the characteristics of the intermolecular energy transfer (IET) are identified as an elementary process of

_____
[a)]Electronic mail: ohara@ifs.tohoku.ac.jp

heat conduction. Such a study would enable us to explore not only the thermal conductivity of liquids, but also their microscale energy-transfer characteristics based on our knowledge of the microscopic structure of fluid. This may lead to a new technology of active control of energy-transfer characteristics by changing the fluid structure.

In the present paper, the energy transfer between molecules in liquid water was analyzed, and the contribution to macroscopic heat conduction was determined. The role of the hydrogen bond in the heat conduction process is also discussed. In the next section, the intermolecular energy exchange rate (IEER) between two molecules is defined using power acting on the two molecules according to the intermolecular force and velocity of molecules. An ordinary equilibrium MD simulation was performed and the observed IEER was analyzed. In Sec. III, heat conduction characteristics under a temperature gradient were estimated by utilizing the characteristics of the IEER, and the role of the hydrogen bond in the heat conduction process was determined. In Sec. IV, MD simulations of heat conduction under a constant temperature gradient were used to verify the estimation as defined in Sec. III. The results are discussed in Sec. V.

II. ENERGY EXCHANGE BETWEEN MOLECULES

In the present study, the magnitude of the energy exchange between two molecules is evaluated as follows under the pair-potential approximation.

With regard to the translational motion of a molecule i, the rate of increase of kinetic energy, $\dot{E}_{k,i}^{\text{trans}}$, equals the power due to the force acting on the molecule i,

$$\dot{E}_{k,i}^{\text{trans}} = \frac{\partial E_{k,i}^{\text{trans}}}{\partial t} = \mathbf{F}_i \cdot \boldsymbol{\nu}_i . \tag{1}$$

Here t and $\boldsymbol{\nu}_i$ denote the time and velocity vector of molecule i, respectively. Superscript trans and subscript k represent the translational motion and kinetic energy, respectively. The force vector acting on the molecule i, $\mathbf{F}_i$, is a resultant force from intermolecular forces between molecule i and all the other molecules j, $\mathbf{F}_{ij}$. Then, $\dot{E}_{k,i}^{\text{trans}}$ is expressed as the sum of the contribution of all the other molecules j,

$$\dot{E}_{k,i}^{\text{trans}} = \mathbf{F}_i \cdot \boldsymbol{\nu}_i = \sum_j \mathbf{F}_{ij} \cdot \boldsymbol{\nu}_i = \sum_j \dot{E}_{k,ij}^{\text{trans}} , \tag{2}$$

where $\dot{E}_{k,ij}^{\text{trans}} = \mathbf{F}_{ij} \cdot \boldsymbol{\nu}_i$. With regard to rotational motion of the molecule, the expression given below is derived in a similar way to Eq. (2),

$$\dot{E}_{k,i}^{\text{rot}} = \sum_j \mathbf{N}_{ij} \cdot \boldsymbol{\omega}_i = \sum_j \dot{E}_{k,ij}^{\text{rot}} , \tag{3}$$

where $\dot{E}_{k,ij}^{\text{rot}} = \mathbf{N}_{ij} \cdot \boldsymbol{\omega}_i$. Here, $\mathbf{N}_{ij}$ and $\boldsymbol{\omega}_i$ are the torque acting on the molecule i due to j and the angular velocity of the molecule i, respectively. Superscript rot represents the rotational motion.

The increase in the kinetic energy of a molecule i resulting from the interaction between two molecules i and j is evaluated by the above $\dot{E}_{k,ij}^{\text{trans}}$ and $\dot{E}_{k,ij}^{\text{rot}}$. In addition to the increase in the kinetic energy, changes in the intermolecular

potential energy should also be included. The rate of increase in the intermolecular potential energy between the two molecules i and j, $\dot{E}_{p,ij}$, follows the equation below,

$$\dot{E}_{k,ij}^{\text{trans}} + \dot{E}_{k,ji}^{\text{trans}} + \dot{E}_{k,ij}^{\text{rot}} + \dot{E}_{k,ji}^{\text{rot}} + \dot{E}_{p,ij} = 0, \tag{4}$$

where $E_{p,ij}$ is the intermolecular potential energy and $\dot{E}_{p,ij} = \partial E_{p,ij}/\partial t$. In the present study, the rate of increase in the intermolecular potential energy, $\dot{E}_{p,ij}$, is divided into the two contributions, the contribution of the translational motion of molecules and that of the rotational motion of molecules. The two contributions, denoted by $\dot{E}_{p,ij}^{\text{trans}}$ and $\dot{E}_{p,ij}^{\text{rot}}$, respectively, are defined as follows:

$$\dot{E}_{p,ij}^{\text{trans}} = -(\dot{E}_{k,ij}^{\text{trans}} + \dot{E}_{k,ji}^{\text{trans}}),$$
$$\dot{E}_{p,ij}^{\text{rot}} = -(\dot{E}_{k,ij}^{\text{rot}} + \dot{E}_{k,ji}^{\text{rot}}), \tag{5}$$

where $\dot{E}_{p,ij}^{\text{trans}} + \dot{E}_{p,ij}^{\text{rot}} = \dot{E}_{p,ij}$. The rates of increase in the intermolecular potential energy, $\dot{E}_{p,ij}^{\text{trans}}$ and $\dot{E}_{p,ij}^{\text{rot}}$, are distributed to the two molecules i and j equally. Now the intermolecular energy exchange rate (IEER) from a molecule j to a molecule i, which is denoted by $\dot{q}_{ij}$, is evaluated by a sum of the increase rate of kinetic energy of the molecule i due to j and a half of the increase rate of intermolecular potential energy between molecules i and j as follows:

$$\dot{q}_{ij}^{\text{trans}} = \dot{E}_{k,ij}^{\text{trans}} + \tfrac{1}{2}\dot{E}_{p,ij}^{\text{trans}} = \tfrac{1}{2}(\dot{E}_{k,ij}^{\text{trans}} - \dot{E}_{k,ji}^{\text{trans}}),$$
$$\dot{q}_{ij}^{\text{rot}} = \dot{E}_{k,ij}^{\text{rot}} + \tfrac{1}{2}\dot{E}_{p,ij}^{\text{rot}} = \tfrac{1}{2}(\dot{E}_{k,ij}^{\text{rot}} - \dot{E}_{k,ji}^{\text{rot}}). \tag{6}$$

In the present paper, $\dot{q}_{ij}^{\text{trans}}$ and $\dot{q}_{ij}^{\text{rot}}$ are called the translational IEER and the rotational IEER, respectively. The expression of Eq. (6) gives that $\dot{q}_{ij} = -\dot{q}_{ji}$, which is suitable to our image that a certain amount of energy transfers from a molecule to the other.

To examine characteristics of the IEER, MD simulations were performed. The exchange of energy between molecules always occurs even in conditions of thermal equilibrium, although the time average of the IEER is zero. Therefore, an ordinary equilibrium MD simulation is enough to examine the magnitude of the IEER.

In the MD simulation, water molecules modeled by the SPC/E potential,[10] one of the most successful potential models for liquid water using a rigid molecule, were arranged in a cubic cell with a three-dimensional periodical boundary condition. Long-range electrostatic forces were treated by the Ewald summation technique.[11]

Simulations were performed mainly for saturated liquid at several temperatures. The saturated liquid density of the SPC/E water is given by Guissani and Guillot,[12] and the critical point was determined in their report to be 651.7 K and 326 kg/m³. The simulations were performed at several temperatures, ranging from a temperature slightly above the triple point to a temperature slightly above the critical point, as shown in Table I. The number of molecules arranged in the basic cell is also indicated in Table I.

For each condition, 40 000 steps with constant total energy were devoted for analysis after aging of the system for

TABLE I. Simulated state points and numbers of molecules arranged in the system.

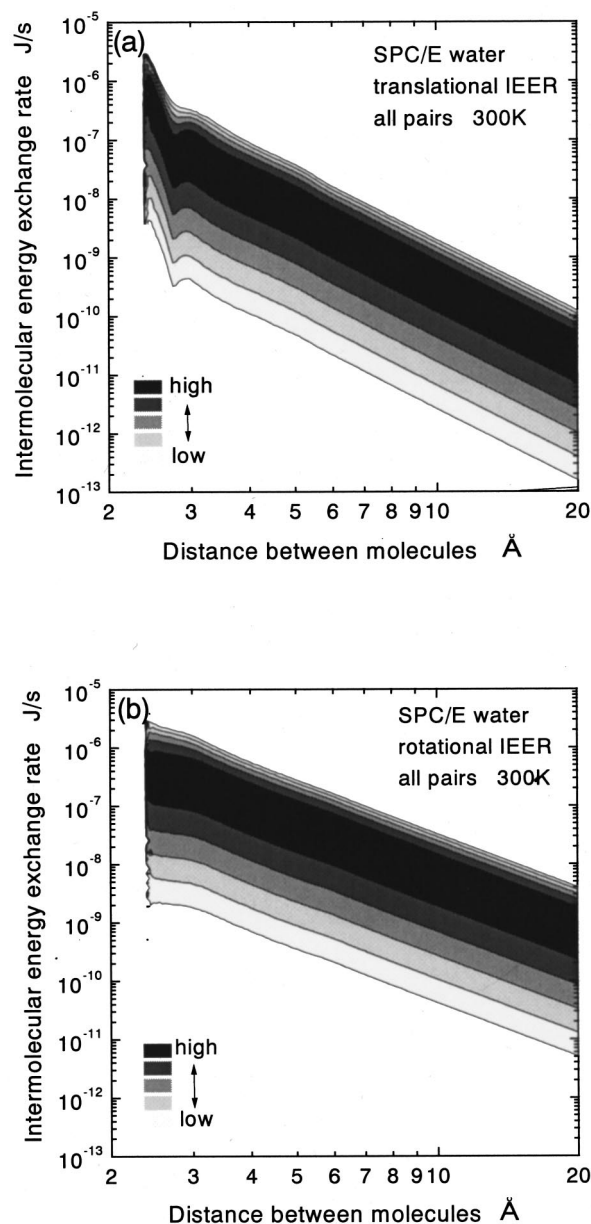| Target temperature K	Resulting temperature K	Density kg/m^3	Number of molecules
300	303	998	2048
350	353	970	2000
400	399	930	1900
450	452	870	1800
500	505	800	1600
550	551	710	1500
600	597	580	1200
650	655	330	700
660	661	290	1024

FIG. 1. Probability distribution of the intermolecular energy exchange rates (IEERs) between water molecules at $T = 300$ K as a function of their distance. (a) Translational IEER (upper figure), (b) rotational IEER (lower figure).

20 000 steps while keeping the temperature constant. The applied time step was 0.25 fs. During the simulations, the IEERs, $\dot{q}_{ij}^{\text{trans}}$ and $\dot{q}_{ij}^{\text{rot}}$, were acquired for each molecular combination at each step. The distances between the two molecules were also measured simultaneously. Histograms were obtained separately for pairs of hydrogen-bonded molecules and those having no hydrogen bond between them. The hydrogen bond was defined to exist between molecules whose intermolecular potential energy was lower than 2.0×10^{-20} J.

The probability distributions of the translational IEER and the rotational IEER between water molecules at $T = 300$ K are shown in Fig. 1. The figures indicate the probability of the IEER when the two molecules are at a certain distance apart. Information of the radial distribution of molecules is eliminated. Since the distributions for positive and negative values are symmetrical, only the distributions of positive values are shown in the figure.

These results suggest that the IEERs are well correlated with intermolecular distances. As shown in Fig. 1(a), a kink was found in the distributions of the translational IEER, which is thought to be due to the characteristics of the hydrogen bond. Figure 2 shows a comparison of the probability distribution of the translational IEER for hydrogen-bonded pairs of molecules and those for nonbonded pairs. These results suggest that the kink in Fig. 1(a) comes from hydrogen-bonded molecules. The intermolecular force between hydrogen-bonded molecules approaches zero at the equilibrium distance ($=2.8$ Å) and then the IEER shows a marked decrease.

Average absolute values of the IEERs at $T = 300$ K are shown in Fig. 3 as a function of intermolecular distance. The translational and rotational IEERs are plotted in the figure for hydrogen-bonded molecules and nonbonded molecules. The translational IEER is greater than the rotational IEER only around the closest distance between the molecules (~ 2.5 Å). At greater distances, the rotational IEER is higher than the translational IEER. Also, the slope of the decrease of the rotational IEER is less than that of the translational IEER. Therefore, the difference between the rotational IEER and the translational IEER is larger at greater distances.

At higher temperatures, the translational and rotational IEERs are larger for both the hydrogen-bonded pairs and the nonbonded pairs. The average values are proportional to the square root of the temperature, since average velocity of the molecules increases according to the increase in temperature. The curves in Fig. 3 maintain their shapes as the temperature increases from $T = 300$ to 660 K. However, the kink in the curve of the translational IEER that is formed due to hydrogen-bonded molecules is less remarkable at higher temperatures.

III. ESTIMATION OF HEAT CONDUCTION CHARACTERISTICS

The IEERs described in Sec. II are instantaneous values, but the effective amount of energy transferred between two molecules is given by the integration of the IEERs over a certain period of time. In the thermal equilibrium state simu-
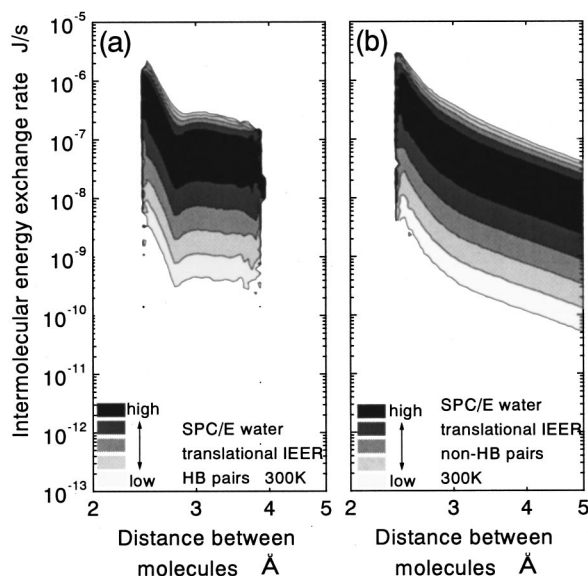
FIG. 2. Probability distribution of the translational intermolecular energy exchange rates (IEERs) at $T = 300$ K as a function of intermolecular distance. (a) Between hydrogen-bonded molecules (left figure), (b) between nonbonded molecules (right figure).

lated in Sec. II, there is no dominant direction in the time integration of the IEERs. Therefore, at a macroscopic level, there is not a substantial amount of energy transferred in the liquid. On the other hand, in the case of heat conduction under a macroscopic temperature gradient, a certain direction is thought to become slightly dominant in the IEERs. Therefore, time integration of the IEERs gives a nonzero macroscopic energy transfer.

Understanding the relationship between the IEERs and the rate of the substantial energy transfer between two molecules is the key for evaluating macroscopic heat conduction under a temperature gradient by utilizing the characteristics of the IEERs. Let us consider two molecules in liquid with a macroscopic temperature gradient. Initially, each molecule
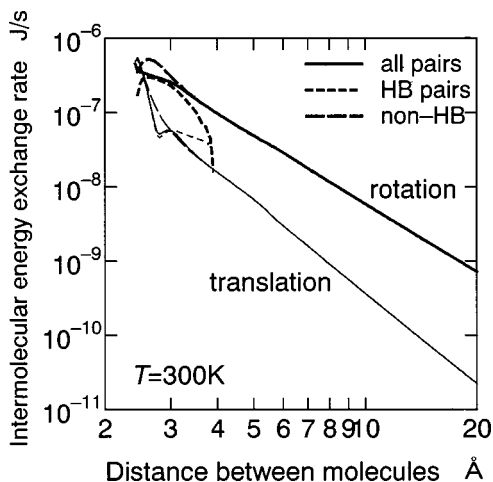

FIG. 3. Average absolute values of the intermolecular energy exchange rate (IEER) at $T = 300$ K observed between hydrogen-bonded water molecules and nonbonded molecules. The translational and rotational IEERs are plotted with thin and thick lines, respectively.

has a different time-averaged kinetic energy according to the temperature gradient. Once their interaction commences, the exchange of kinetic energy between the molecules is repeated with oscillatory IEERs, and the kinetic energy of the two molecules averaged over a sufficient period of time tends to be equal. In the above process, the initial difference in the time-averaged kinetic energy between the molecules due to the macroscopic temperature gradient disappears, and this process is recognized as heat conduction. The rate of the above energy diffusion process is thought to be determined by the IEER. This is true even in cases where the motion of the two molecules is influenced by many other molecules, if we assume that this influence is random and does not have any correlation with the interaction between the two molecules. Based on the above, we assume that the effective rate of IET, $\dot{Q}_{ij}$, which causes macroscopic heat conduction directly, is proportional to the magnitude of the IEER,

$$\bar{\bar{Q}}_{ij} = C \cdot \overline{|\dot{q}_{ij}|} \tag{7}$$

where $^-$ represents the average over molecules.

C is a proportionality constant. $\overline{\bar{Q}}_{ij}$ is much smaller than $\overline{|\dot{q}_{ij}|}$, so that influence of the magnitude of the temperature gradient on the above-mentioned heat conduction process is negligible. Therefore, C is proportional to the macroscopic temperature gradient in the liquid, which is consistent with Fourier's law.

Based on the above supposition, the heat conduction characteristics of liquid under a temperature gradient are analyzed in terms of the IET. This allows us to examine the ratio of the translational and rotational IET and the contribution of hydrogen bonds to the macroscopic heat conduction. Two factors should be considered in determining the rate of macroscopic heat conduction by integrating the contribution of IET. The first factor is number of paths of the IET. Number of molecules j in a shell around a molecule i whose radius and thickness are r_{ij} and Δr_{ij}, respectively, is proportional to $\rho_N g(r_{ij}) r_{ij}^2 \Delta r_{ij}$, where ρ_N and $g(r_{ij})$ denote the number density of molecules and the radial distribution function, respectively. This is substituted for the number of paths of the IET. The other factor is the rate of effective energy transfer per path, where the effective rate of the IET is assumed to be proportional to the IEER, as indicated by Eq. (7). Consequently, an expression for the effective energy transfer rate caused by the IET in liquid according to a temperature gradient is derived as follows. Here, the energy that is transferred in a unit period of time to a molecule i from all the molecules j whose distance from the molecule i is r_{ij}, is denoted by $\bar{Q}_i(r_{ij})$. $\bar{Q}_i(r_{ij})$ is given by

$$\bar{Q}_i(r_{ij}) = C' \rho_N \bar{Q}_{ij}(r_{ij}) g(r_{ij}) r_{ij}^2 \Delta r_{ij}, \tag{8}$$

where $\bar{Q}_{ij}(r_{ij})$ is given by Eq. (7). As it will appear later in Eq. (12), the contribution of the IET between molecules i and j to macroscopic heat flux averaged in a volume should be weighted by r_{ij}. Therefore, $r_{ij}\bar{Q}_i(r_{ij})$ indicate the contribution to macroscopic heat flux. Now, the contribution of the IET of the whole molecular system to heat flux is given as follows:
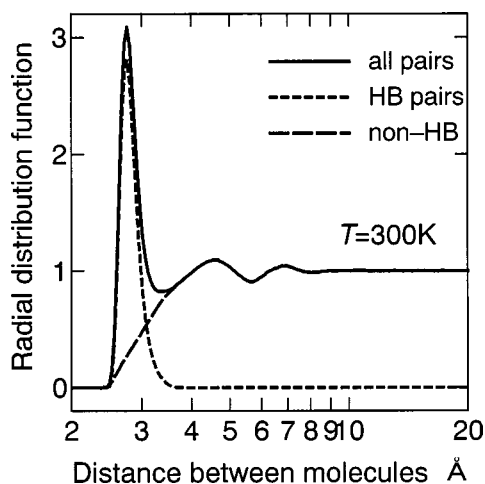
FIG. 4. Radial distribution function $g(r)$ at $T = 300$ K for molecules which are hydrogen bonded to the center molecule, those which are not hydrogen bonded, and all molecules.

$$\bar{Q}(r) = \rho_N \int_{r_{ij}=0}^{r} r_{ij} \bar{Q}_i(r_{ij}) dr_{ij}$$

$$= C' \rho_N^2 \int_{r_{ij}=0}^{r} \bar{Q}_{ij}(r_{ij}) g(r_{ij}) r_{ij}^3 dr_{ij}. \tag{9}$$

$\bar{Q}(r)$ represents the contribution of the IET between molecules whose distance is shorter than r to the macroscopic heat conduction. $\bar{Q}(\infty)$ represents the whole contribution of the IET. They have a dimension of heat flux, i.e., energy per unit period of time and unit area. C' is a proportionality constant.

However, $\bar{Q}(r)$ given by Eq. (9) does not converge even at an infinite value of r because $|\dot{q}_{ij}^{rot}|$ is approximately proportional to r_{ij}^{-3}, as shown in Fig. 3. This fact suggests that contribution of the IET from a long distance is smaller than expected, as the mechanism is discussed later in Sec. V. To incorporate this effect into the model, the $-m$th power of the intermolecular distance is introduced to Eq. (9), which apparently reduces the contribution from a long distance. Now the modified equation is

$$\bar{Q}(r) = C'' \rho_N^2 \int_{r_{ij}=0}^{r} \bar{Q}_{ij}(r_{ij}) g(r_{ij}) r_{ij}^{3-m} dr_{ij}$$

$$= C'' \rho_N^2 \int_{r_{ij}=0}^{r} \bar{Q}_{ij}(r_{ij}) g(r_{ij}) r_{ij}^n dr_{ij}, \tag{10}$$

where $n = 3 - m$. To keep the consistency in dimensions of $\bar{Q}(r)$, C'' has dimensions of $(\text{length})^m$. Since the existence of infinite thermal conductivity is unrealistic, the index n should be much lower than 3. Based on the above discussion, we assume a value of $n = 1$ for the present study. The value of n and the influence of a smaller n on the results will be discussed later.

Using the MD simulations described in Sec. II, the average value of the IEER, $\overline{|\dot{q}_{ij}|}(r_{ij})$, was obtained separately for all pairs, only hydrogen-bonded pairs, and nonbonded pairs of water molecules. Both the translational and rota-

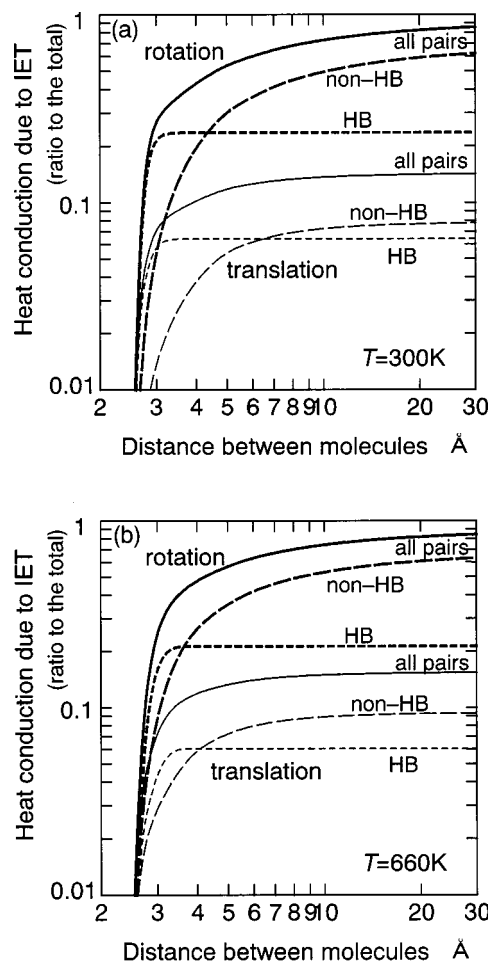
FIG. 5. Heat conduction of water contributed by intermolecular energy transfer (IET) between molecules whose distance is shorter than r, which is given by $\bar{Q}(r)$ in Eq. (10) with $n = 1$. Contribution of hydrogen-bonded pairs of molecules and nonbonded pairs are plotted as ratios to the total value, $\bar{Q}(\infty)$. Contributions of the translational and rotational IET are plotted with thin and thick lines, respectively. (a) $T = 300$ K (upper figure), (b) $T = 660$ K (lower figure).

tional IEERs based on the above classification are shown in Fig. 3. The radial distribution functions are obtained for various temperatures according to the above classification. As an example, those for $T = 300$ K are shown in Fig. 4. Using these functions for Eq. (10) gives us the $\bar{Q}(r)$ for the translational and rotational IET due to the contributions of the hydrogen-bonded pairs and the nonbonded pairs separately.

Figure 5 shows the ratio of $\bar{Q}(r)$ for each contribution to the total $\bar{Q}(\infty)$ for $T = 300$ and 660 K. $\bar{Q}(\infty)$ is evaluated at $r = 30$ Å. As shown in the figure, the IET from molecules farther than 20 Å still contributes to total heat conduction. The contribution of IET from distant molecules cannot be neglected, especially in the rotational energy transfer.

Ratios of the translational and rotational IET to the total $\bar{Q}(\infty)$ and ratios of the IET between hydrogen-bonded molecules and nonbonded molecules are shown in Table II for $n = 1$ and 0. In the case of $n = 1$, it is remarkable that the contribution of hydrogen-bonded molecules is not dominant. This contribution is smaller than that of nonbonded mol-

J. Chem. Phys., Vol. 111, No. 14, 8 October 1999

Energy transfer in liquid water   6497

TABLE II. Estimation of ratio of the translational and rotational intermolecular energy transfer (IET) and contribution of hydrogen-bonded pairs of molecules. These are given by $\bar{Q}(r)$ in Eq. (10) with $r = 30$ Å for $n = 1$ and 0.

$T = 300$ K							
	$n = 1$				$n = 0$		
Translational IET		Rotational IET		Translational IET		Rotational IET	
14%		86%		17%		82%	
HB	non-HB	HB	non-HB	HB	non-HB	HB	non-HB
45%	55%	27%	73%	55%	45%	42%	58%
$T = 660$ K							
	15%		85%		18%		82%
HB	non-HB	HB	non-HB	HB	non-HB	HB	non-HB
39%	61%	25%	75%	45%	55%	35%	65%

FIG. 7. Simulation system for heat conduction under a constant temperature gradient.

ecules, especially in the rotational IET, and decreases further as temperature increases. Over 80% of the total IET is caused by the rotational IET, regardless of temperature. This result is in contrast to a report by Wang and co-workers[7] that the rotational IET does not contribute to heat conduction at all in their studies for carbon dioxide. In the case of $n = 0$, the contribution of hydrogen-bonded molecules increases because the contribution from distant molecules decreases.

An illustration of the temperature dependency of the total heat flux, $\bar{Q}(\infty)$, is plotted in Fig. 6 as a function of temperature. As temperature increases from $T = 300$ K, $\bar{Q}(\infty)$ increases slightly and attains a maximum value at $T = 350$ K. This local maximum results from a balance between two factors; as temperature increases, $\overline{|\dot{q}_{ij}(r_{ij})|}$ increases, which increases $\bar{Q}(r)$, and, simultaneously, number density of the liquid, ρ_N, decreases, which reduces $\bar{Q}(r)$.

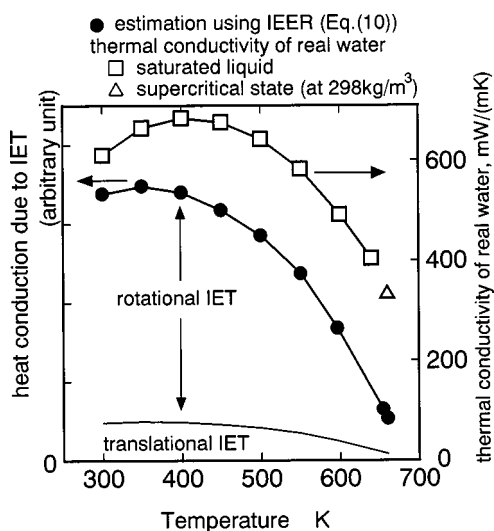The thermal conductivity of real water is also plotted in the figure to compare the temperature dependency. The plots

FIG. 6. Total contribution of intermolecular energy transfer (IET) to heat conduction, $\bar{Q}(\infty)$, given by Eq. (10) with $n = 1$, as a function of temperature. Contribution of the translational and rotational IET are indicated. Thermal conductivity of real water at a saturated liquid state and a supercritical state are also plotted for comparison of temperature dependency. The supercritical state of real water plotted in the figure is the pseudocritical point at 660 K.
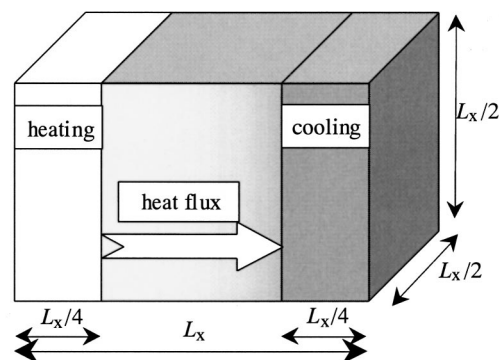
are for saturated liquid at various temperatures and a pseudocritical point at $T = 660$ K and density $\rho = 298$ kg/m^3. A maximum value also appears for real water, but the temperature at maximum thermal conductivity is 400 K, which is higher than that of our estimation by Eq. (10). This tendency can be understood by considering energy transport according to the molecular motion. As discussed in the next section, the heat conduction of fluid is composed of two contributions. One is the IET, which is dominant in low-temperature liquids and has been analyzed in the present paper. The other is caused by the motion of molecules that transports kinetic and potential energy by themselves. Thus, the thermal conductivity of real water plotted in Fig. 6 indicates the combined contributions of the IET and energy transport by the molecules themselves. The former was evaluated by Eq. (10) and plotted in the figure. The latter is considered to be larger at higher temperature due to the increase in the motion of molecules. Therefore, this contribution shifts the maximum point toward higher temperatures. This suggests that the estimation of the IET in the present study is consistent qualitatively with the experimental observation of real water.

IV. MD SIMULATION OF HEAT CONDUCTION UNDER A CONSTANT TEMPERATURE GRADIENT

In order to test the validity of the estimation described in Sec. III, nonequilibrium MD (NEMD) simulations of heat conduction were performed. In order to determine the thermal conductivity, most NEMD studies introduce a fictitious field to drive heat flux[13] by adding special terms to the equation of molecular motion. The alternative method is to introduce to the system a real temperature gradient and heat flux. This can be achieved by keeping the temperature at each end of the calculation cell at different levels[14] or supplying a certain amount of energy to one end region of the calculation cell and simultaneously withdrawing the same amount of energy from the other end region.[8] The method for introducing a fictitious field may not be appropriate for the present study because the influence of the fictitious field on the characteristics of IET is not fully understood. Therefore, we used a real temperature gradient in the system.

The applied system is represented in Fig. 7. A rectangular cell with a square cross section contains 1024 water molecules modeled by the SPC/E potential. The temperature gra-

TABLE III. Simulation condition for the steady heat conduction.

T_H K	T_L K	ρ kg/m^3	L_x Å	Number of steps
320	300	998	50	2 million
680	640	290	75	1 million

TABLE IV. Results of the simulation: Thermal conductivity and ratio of the intermolecular energy transfer (IET) to the total heat flux, including the contribution of molecular motion.

T K	Thermal conductivity W/(mK)		Ratio of IET
	Result	Real water	
300–320	0.95	0.6	96%
640–680	0.28	0.32	45%

dient is given in the x direction. The length of the cell in the x direction is twice the length of the y and z direction. Periodic boundary conditions are applied in the y and z direction. For each end face of the basic cell in the x direction, forces from the face acting on the molecules prevent them from escaping the cell passing through the end face. For this purpose, the Lennard-Jones (12-6) potential was applied to all of the molecules according to the distance between the molecule and the end face.

The simulation conditions are shown in Table III. A temperature gradient was formed in the liquid, with heating and cooling regions set at each end of the rectangular cell. The velocity of all water molecules in these regions was scaled during the simulation to maintain the average temperature at T_H and T_L. During the 100 000 step aging process of the system, the center region between the heating and cooling regions was divided into ten slabs, and the average temperature of each slab was maintained by velocity scaling, forming the temperature gradient. After aging of the system, a simulation of one or two million steps was performed for two conditions. The data from the initial 100 000 steps were abandoned and next 900 000 steps or 1 900 000 steps were analyzed. During the simulation, temperature controls were applied to each slab for 10 steps at every 1000 steps.

In the simulation, the most important factor affecting heat conduction is the direct interaction between molecules that are less than 20 Å apart. Therefore, the Ewald summation technique was not used, and the intermolecular forces were evaluated only for images of minimum distance, which saves the CPU more than 20% of the time it takes to calculate the intermolecular forces.

In many reports in which heat flux is evaluated by MD simulations, the heat flux is calculated based on the following equation:

$$J_{Q,x}S_{yz} = \sum_i (E_i/1)\frac{\nu_{x,i}}{|\nu_{x,i}|} + \frac{1}{2}$$
$$\times \sum_i \sum_j (\boldsymbol{\nu}_i \cdot \mathbf{F}_{ij} + \boldsymbol{\omega}_i \cdot \mathbf{N}_{ij})\frac{x_{ij}}{|x_{ij}|}. \quad (11)$$

Here, $J_{Q,x}$ and S_{yz} represent heat flux and the area of control surface which is perpendicular to the heat flux, respectively. E_i represents energy held by molecule i, which is given by the sum of the kinetic and potential energy. The first term on the right side of Eq. (11) represents the energy transport caused by the motion of the molecules itself and the Σ is the sum of the energy transport of all molecules which pass through the control surface in a unit period of time. The second term represents the energy transferred through the control surface due to the interaction between molecules,

which is equivalent to the definition of the IEER. The Σ is the sum of the IET between all pairs of molecules which hold the control surface between them.

In most cases, the following equation is applied for practical use, which is derived by integrating Eq. (11) over a certain length in the direction of the heat flux, x,

$$J_{Q,x}V = \sum_i E_i\nu_{x,i} + \frac{1}{2}\sum_i\sum_j x_{ij}^*(\boldsymbol{\nu}_i \cdot \mathbf{F}_{ij} + \boldsymbol{\omega}_i \cdot \mathbf{N}_{ij}). \quad (12)$$

Equation (12) gives the heat flux averaged over a control volume, V. In the present simulation, a control volume with a width of 8 Å is located at the center of the cell in the x direction and the heat flux is evaluated by Eq. (12). The first Σ on the right side of Eq. (12) is the sum of all molecules that are contained in the control volume. The $\Sigma\Sigma$ is the sum of all pairs of molecules with the condition that the line connecting the two molecules penetrates any yz plain included in the control volume. In cases where only part of the connecting line is contained in the control volume, i.e., one or both of the two molecules are located out of the control volume, then x_{ij}^* is x length of the part of the connecting line contained in the control volume.

The thermal conductivity obtained from the simulations and the ratio of the contribution of molecular interaction given by the second term on the right side of Eq. (12) to the total heat flux are shown in Table IV. There is fair agreement between the simulated results and the data for real water. The contribution of the IET is 0.91 W/(mK) at $T=300$–320 K and 0.13 W/(mK) at $T=640$–680 K. The ratio of these values is 7:1. As shown in Fig. 6, the predicted value from Eq. (10) of the ratio of the IET at $T=300$ K to the IET at $T=660$ K is 6.4. There is good agreement between these two values, which suggests that the temperature dependency of the heat conduction due to the IET is predicted by Eq. (10) satisfactorily.

Although direct verification of the validity of Eqs. (7) and (10) would be ideal, we found that the present simulation of one or two million steps is not sufficient for that purpose. At least several million steps may be required to obtain reliable data as a function of intermolecular distance. Therefore, we obtained the ratio of the translational and rotational IETs to their total, and further determined the relative contributions of the hydrogen-bonded molecules and nonbonded molecules. These data correspond to those of Table II and are shown in Table V.

The results predicted by Eq. (10) shown in Table II and the simulated results in Table V agree qualitatively in the following manner. The rotational IET is dominant in the total

TABLE V. Results of the simulation: Ratio of the translational and rotational intermolecular energy transfer (IET) and contribution of hydrogen-bonded pairs of molecules.

$T = 300{-}320$ K			
Translational IET		Rotational IET	
35%		65%	
HB	non-HB	HB	non-HB
59%	41%	22%	78%
$T = 640{-}680$ K			
22%		78%	
HB	non-HB	HB	non-HB
41%	59%	16%	84%

IET at both temperatures. The contribution of the IET between hydrogen-bonded molecules is limited especially in the rotational IET, and this contribution decreases as temperature increases. These characteristics were observed in the simulation and were successfully predicted by Eq. (10), as shown in Table II.

Generally, the predicted results with $n = 1$ agree with the simulated results better than the predicted results with $n = 0$. However, especially for the case of $T = 300$ K, there are two major quantitative discrepancies between the predicted results with $n = 1$ and the simulated results. One is the ratio of the translational and rotational IETs to the total IET. The translational IET is underestimated in the prediction. The other discrepancy is the underestimation of the ratio of the contribution of hydrogen-bonded molecules for the translational IET at $T = 300$ K, while the contribution of hydrogen-bonded molecules for the rotational IET was accurately predicted. These problems will be discussed in the next section.

V. DISCUSSION

In the present paper, heat conduction in liquid water due to the interaction between molecules has been modeled using the concept of IET based on the characteristics of the IEER and the effective rate of IET. Using our model, the predicted results agreed qualitatively with simulated results. In order to improve our predictions, we will discuss modifications to our model.

It was stated in Sec. III that the index n in Eq. (10) must be lower than 3, although two possible factors suggest that $n = 3$. A good correlation was found when the predicted value from Eq. (10) when $n = 1$ (Table II) and the results of the heat conduction simulation (Table V) were compared. One exception was the ratio of the contribution of hydrogen-bonded molecules and nonbonded molecules to the total translational IET at $T = 300$ K. These facts suggest that there is a mechanism to cancel the energy transfer between molecules that are far apart, which reduces $r_{ij}^n \bar{Q}_{ij}(r_{ij})$ in Eq. (10) when r_{ij} is large. One possible mechanism is described below. Figure 8 is a sketch of the radial distribution function. Let us think about the translational IET between a center molecule, C, and surrounding molecules in the first and second neighbor shells, 1 and 2, respectively. The effective rate of the translational IET between molecules C and 1, $\bar{Q}_{C1}$, is positive on average as well as the translational IET between molecules 1 and 2, $\bar{Q}_{12}$. Here the word positive means that
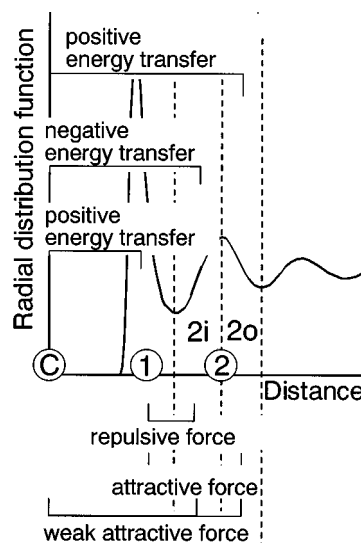

FIG. 8. Influence of liquid structure on the effective intermolecular energy transfer.

the energy transfer is in the same direction as macroscopic heat conduction, i.e., from the high-temperature side to the low-temperature side. In contrast to the effective IET between neighbor molecules, the effective IET between C and 2, $\bar{Q}_{C2}$, is rather complicated. The intermolecular force between C and 2, $\mathbf{F}_{C2}$, has the same sign as that between 1 and 2, $\mathbf{F}_{12}$, when molecule 2 is in the outer half region of the second neighbor shell indicated in Fig. 8 as 2o, i.e., they are both attractive forces. On the other hand, $\mathbf{F}_{C2}$ and $\mathbf{F}_{12}$ have different signs in the inner half region of the second neighbor shell indicated in Fig. 8 as 2i.

$\mathbf{F}_{12}$ has much stronger influence on the motion of 2 than $\mathbf{F}_{C2}$ and leads to a positive effective IET, $\bar{Q}_{12}$. Under such circumstances, it is likely that $\bar{Q}_{C2}$ is positive when $\mathbf{F}_{C2}$ has the same sign as $\mathbf{F}_{12}$, and $\bar{Q}_{C2}$ is negative when $\mathbf{F}_{C2}$ has a different sign than $\mathbf{F}_{12}$. Consequently, $\bar{Q}_{C2}$ takes positive and negative values in the outer and inner half regions of the second neighbor shell, respectively, and they practically cancel each other out. This phenomenon occurs only for the translational IET at low temperatures, where a firm liquid structure exists.

If the above phenomenon is taken into account in the prediction based on the effective rate of IET, this reduces the translational IET from molecules outside of the first neighbor shell. This makes the contribution of hydrogen-bonded molecules to the translational IET relatively larger, and one discrepancy between the predicted value (Table II) and the simulated result (Table V) mentioned in Sec. IV, which underestimated the contribution of hydrogen-bonded molecules, disappears.

On the other hand, the other discrepancy (the small contribution of the translational IET relative to the rotational IET) between the predicted value and the simulated result is not solved by modifying the predicted value in the above-mentioned manner. One possible reason for this discrepancy is that the same constant C was applied in Eq. (7). The os-

cillations of the translational and rotational IEERs have different frequencies so that the energy transfer phenomenon in the process of oscillatory intermolecular energy exchange may have a different time constant. However, further research will be needed to determine C quantitatively.

According to the considerations in Sec. III, the index n in Eq. (10) should equal 3, if the interactions between all pairs of molecules occur independently. Instead, using $n = 0-1$ gives a predicted result that agrees with the simulated results. These results suggest the existence of a mechanism which reduces n virtually even in the rotational IET. Although this may be due to cancellation of the contribution of distant molecules, further work will be required to elucidate the mechanism.

VI. CONCLUSION

Intermolecular energy transfer (IET) between water molecules, which is the dominant mechanism of heat conduction in low-temperature liquid water, was analyzed. The intermolecular energy exchange rate (IEER) was defined for the translational and rotational IET and its magnitude was determined by MD simulations as a function of intermolecular distance for hydrogen-bonded molecules and other types of intermolecular interactions. Based on the supposition that the effective rate of the IET which contributes to macroscopic heat conduction under a temperature gradient is proportional to the IEER, heat conduction characteristics in liquid water were analyzed. The results suggest that the rotational IET is dominant and contribution of IET between hydrogen-bonded molecules is limited. These results were verified qualitatively by MD simulation of heat conduction under a constant temperature gradient.

A direct verification of Eqs. (7) and (10) by the MD simulations is now being performed for simple fluid and water. The results will be reported in the near future with newer models which take into account the influence of liquid structure on the IET.

[1] Liu Ming, J. Davidsson, and S. Nordholm, J. Chem. Phys. **104**, 9001 (1996).
[2] R. Vogelsang, C. Hoheisel, and G. Ciccotti, J. Chem. Phys. **86**, 6371 (1987).
[3] P. J. Gardner, D. M. Heyes, and S. R. Preston, Mol. Phys. **73**, 141 (1991).
[4] R. Vogelsang, C. Hoheisel, G. V. Paolini, and G. Ciccotti, Phys. Rev. A **36**, 3964 (1987).
[5] G. V. Paolini, G. Ciccotti, and C. Massobrio, Phys. Rev. A **34**, 1355 (1986).
[6] D. J. Evans and S. Murad, Mol. Phys. **68**, 1219 (1989).
[7] B. Y. Wang, P. T. Cummings, and D. J. Evans, Mol. Phys. **75**, 1345 (1992).
[8] T. Ikeshoji and B. Hafskjold, Mol. Phys. **81**, 251 (1994).
[9] B. Hafskjold, T. Ikeshoji, and S. K. Ratkje, Mol. Phys. **80**, 1389 (1993).
[10] H. J. C. Berendsen, J. R. Grigera, and T. P. Straatsma, J. Phys. Chem. **91**, 6269 (1987).
[11] M. P. Allen and D. J. Tildesley, *Computer Simulation of Liquids* (Oxford University Press, 1989), pg. 159.
[12] Y. Guissani and B. Guillot, J. Chem. Phys. **98**, 8221 (1993).
[13] P. T. Cummings and D. J. Evans, Ind. Eng. Chem. Res. **31**, 1237 (1992).
[14] J. M. Kincaid and B. Hafskjold, Mol. Phys. **82**, 1099 (1994).